nature research

https://doi.org/10.1038/s41558-020-00918-2

Supplementary information

Increasing ocean stratification over the past half-century

In the format provided by the authors and unedited

Supplementary Information

Increasing Ocean Stratification Over the Past Half Century

Guancheng Li[1,2,3], Lijing Cheng[1,2,3], Jiang Zhu[1,2,3], Kevin E. Trenberth[4], Michael E. Mann[5], John P. Abraham[6]

[1]International Center for Climate and Environment Sciences, Institute of Atmospheric Physics, Chinese Academy of Sciences, Beijing, China, 100029. [2]Center for Ocean Mega-Science, Chinese Academy of Sciences, Qingdao, China, 266071. [3]University of Chinese Academy of Sciences, Beijing, China. [4]National Center for Atmospheric Research, PO Box 3000, Boulder, CO 80307, USA. [5]Department of Meteorology and Atmospheric Science, Department of Geosciences, and Earth and Environmental Systems Institute, Pennsylvania State University, Pennsylvania, USA. [6]School of Engineering, University of St. Thomas, 2115 Summit Ave., St Paul, MN 55105, USA. Email: chenglij@mail.iap.ac.cn; jzhu@mail.iap.ac.cn

Nature Climate Change
The material includes 2 sections with 3 figures, 4 tables

Supplementary Material

1. A brief evaluation on data products.

In addition to the IAP data, several other products (i.e. NCEI, EN4, Ishii, ORAS4) are also used to estimate the long-term ocean stratification changes since 1960. However, as serious discrepancies are found among products, it is worthwhile to have a brief summary for the data evaluation.

1.1 Surface and 200m temperature change and their impact on stratification calculation following IPCC-AR5 method.

As IPCC-AR5 contrasted the temperature between the sea surface (SST) and 200m (T200) to approximate the ocean stratification[1], we first investigate SST and T200 changes since 1960 from different products in Extended Data Fig. 2.

EN4/Ishii/IAP/ORAS4/NCEI SST changes are compared with three independent and widely accepted surface-observations (ERSST, COBE2 and HadSST3) (Extended Data Figs. 2a and 2b). EN4, NCEI, and ORAS4 show ~39%, ~10% and ~20% smaller SST trends over the 1960-2018 period compared to the ensemble mean of three observational SST products. This indicates a major bias in these data. Ishii shows the best consistency compared with independent data, but it has already used COBE analysis in the reconstruction[2]. IAP data shows a slightly stronger trend than ERSST/COBE2/HadSST3, that is partly attributed to how ice-covered regions are handled.

The spatial distribution of long-term SST trends over the 1971-2010 period provides more insights into the data differences or data biases (Extended Data Fig. 3). It appears that EN4 shows a more distinctive pattern than other data. The major differences appear in the Southern oceans, tropical Eastern Pacific Ocean, and tropical Western Atlantic Ocean. This indicates that EN4 data suffered from major biases near the surface. NCEI is unphysically spotty, which is associated with an over-simplified assumption of isotropy in spatial covariance used in their mapping method[3].

For T200, EN4/NCEI/ORAS4 also show a smaller warming rate than the IAP data (31%/30%/59% smaller than IAP) (Extended Data Figs. 2c and 2d). IAP and Ishii are consistent with each other with a trend difference of less than 4% from 1960 to 2018, likely because they have been corrected for the “conservative bias” (which will be discussed below).

This comparison reveals the smaller warming trends for EN4/NCEI/ORAS4 data than other products, implying the existence of data bias. To further test the impact of the data difference on the stratification estimate using IPCC-AR5 method, we included an additional sensitivity test as follows.

(1) Impact of surface data

We use the same IAP temperature at 200m but different surface datasets to test the impact of surface data on stratification calculation (Supplementary Fig. 1a). Using EN4 data gives ~0% increase in stratification within 1971-2010 (adapting to the IPCC-AR5 time period), while other data give positive estimates ranging from 2.8~5.3%. This explains why SROCC gives weaker estimates of stratification change when using the EN4 data than this study and IPCC-AR5. NCEI data (used in IPCC-AR5) also shows weaker change (~2.8%) than Ishii/IAP/ORAS4/ERSST/COBE2/HadSST3 (3.1~5.3%), which explains the weaker stratification trend in IPCC-AR5 compared to this study.

(2) Impact of 200m data

To test the impact of data difference at 200m on stratification estimation, we use the same SST time series (ensemble mean of three independent SST products) but different 200m temperature from different products. During the IPCC-AR5's 1971-2010 period, IAP/Ishii results are similar to each other, but weaker than EN4/ORAS4/NCEI by ~1% (Supplementary Fig. 1b). This indicates that inter-data difference at 200m plays a secondary role for the difference of stratification estimates if the IPCC-AR5's method is adopted.

1.2 "Conservative bias" in previous data products

Beyond the surface and 200m layers, at the ocean volume of the upper 2000m, data biases in traditional data products is an issue that prevents us giving more weights to these data. There is a long-standing issue of "conservative bias" in many products that has been extensively studied before[4-7]. As explicitly stated regarding the EN4 data[8]: "*It is important to note that the analyses will relax to climatology in the absence of any observations. Care must therefore be taken if using the analyses for applications such as identifying trends in temperature or salinity, because a trend may be unrealistic if analyzing periods when there were no observations.*". As this bias assumes "no data, no signal", it leads to an underestimation of long-term ocean warming trends in previous objective analysis products including the Ishii/NCEI/EN4 data[4,6]. A simple illustration of this bias can be found in Supplementary Fig. 2 which shows the difference of the temperature field between 1970 and 1990 at a 700m depth for EN4, Ishii, NCEI, and IAP data respectively. The near-zero anomalies are evident in data sparse regions such as the Southeast Pacific Ocean for EN4/Ishii/NCEI data. This is an indicator of the conservative bias.

IPCC-AR5 actually realized this "conservative bias" in their assessment of ocean heat content: "*Generally the smaller trends are for estimates that assume zero anomalies in areas of sparse data, as expected for that choice, which will tend to reduce trends and variability. Hence the assessment of the Earth's energy uptake (Box 3.1) employs a global UOHC estimate (Domingues et al., 2008) chosen because it fills in sparsely sampled areas and estimates uncertainties using a statistical analysis of ocean variability patterns*" (AR5-chapter-3)[1]. Therefore, IPCC-AR5's ocean heat content estimate did not use EN4, NCEI and Ishii data, but this choice was not applied in the calculation of stratification in both AR5 and SROCC. So, a major update is needed. The need for a major update is the motivation for this present study.

Note that as Ishii incorporated a major update to their data in 2017, explicitly accounting for this bias[9], the new Ishii data used in this study is similar to IAP for global average metrics. However, some issues still occur in the Southern Oceans, because they have applied a global correction to the "conservative bias" but the local signals are still biased[2,10] (Supplementary Fig. 2). More discussion on temperature and salinity products can be found in previous studies[6,10-12].

In summary, all these considerations bring us to recognizing the IAP data as a more reliable estimate compared to other datasets. It provides the best estimate so-far because it suffers less from bias.

2. Uncertainty associated with vertical sampling.

Over the past half century, with the evolution of the ocean observation system, the vertical resolution of temperature and salinity observations have experienced a significant change at all depths since the 1960s (see Extended Data Fig. 4 and Fig. 1 in Cheng and Zhu [13]). For example, the global averaged vertical resolution of *in situ* temperature observations increased substantially from 60~75m pre-1992 to 10~49m post-1992 at 400-700-m depths. This was the result of the wide use of deep-reaching eXpendable BathyThermographs (XBTs). During 2000-2005, there is a temporary decrease in vertical resolution due to the decrease of XBT deployment, which slowly recovered with the Argo system after 2005 (Extended Data Fig. 4a). For salinity observations (Extended Data Fig. 4b), at around 1990, there is a clear increase of vertical resolution below 200m due to more operations of conductivity-temperature-depth (CTD) instruments. An apparent resolution increase for both temperature and salinity observations since ~2005 reveals the impact of Argo network.

During the production of gridded datasets (except ORAS4, where a data assimilation method is used), a vertical interpolation method has been routinely used to standardize the vertical levels of observations (Supplementary Table 2). Inaccuracy during vertical interpolation can lead to additional errors and cause inconsistencies among products.

However, the uncertainty associated with vertical resolution in observations and vertical interpolation method haven't been explicitly taken into account in all of the current available products. Here, in IAP data production framework, we quantify their impacts by a "vertical subsample test".

2.1 Vertical subsample test.

The "vertical subsample test" used here builds upon previous efforts of Cheng and Zhu [13] for the vertical subsampling, and on Cheng and Zhu [14] and Cheng, et al. [5] for the horizontal subsampling. This approach is also recommended by the scientific community according to Allison et al. [15] (it has been named the "synthetic profiles" method). This test includes five steps (illustrated in Extended Data Fig. 5), which are articulated below:

Step-1: Construction of 12 high-vertical-resolution temperature/salinity (T/S) climatologies. To this end, all high-vertical-resolution observational profiles (with mean vertical resolution <5 m in the upper 200m, <10m within 200-1000m and <25m within 1000-2000m) obtained during 1960 to 2018 are collected together. These high-resolution profiles are then interpolated to 1m vertical layers from 0m to 2000m, and then averaged in each 1° by 1° grid cell to create a monthly 1° by 1° grid climatology (denoted as: **high-vert-res-clim**). 12 monthly climatologies are available for both T and S, and these climatologies do not involve any time variation.

Step-2: Horizontal re-sampling. We subsample each **high-vert-res-clim** according to the past horizontal observation masks since 1960, selected every 30 months. from 1960 to 2017, in both summer and winter (24 months in total). Thus, each static field of **high-**

vert-res-clim corresponds to 24 “horizontal subsampled fields” spanning from 1960 to 2017.

Step-3: Vertical re-sampling. Two different subsets of data are created separately based on the horizontal subsampled fields from Step-2. First, we further resample the “horizontal subsampled fields” according to the observational vertical masks (the resultant fields are denoted as **obs-vert-res**). These fields mimic the real ocean observations. Second, no vertical re-sampling is applied to the “horizontal subsample fields”, which forms a high vertical resolution fields (denoted as: **high-vert-res**). The only difference between the **obs-vert-res** and **high-vert-res** is the vertical resolution.

Step-4: Vertical interpolation and mapping. The **obs-vert-res** fields are interpolated to standard levels by three vertical interpolation methods separately (linear, spline, and Reiniger-Ross method). The three interpolated fields are then mapped using the IAP method to obtain three gridded datasets with complete spatial coverage (denoted as: $\mathbf{T^{L}_{obs\text{-}vs}}$ for linear, $\mathbf{T^{R}_{obs\text{-}vs}}$ for Reiniger-Ross, $\mathbf{T^{S}_{obs\text{-}vs}}$ for spline). The **high-vert-res** fields do not need any interpolation and are directly input into the mapping method, and result in another gridded product: $\mathbf{T_{high\text{-}vs}}$.

Step-5: Calculation of vertical sampling error (VSE). By comparing the three gridded products based on **obs-vert-res** ($\mathbf{T^{L}_{obs\text{-}vs}}$, $\mathbf{T^{R}_{obs\text{-}vs}}$, $\mathbf{T^{S}_{obs\text{-}vs}}$) with the **high-vert-res** ($\mathbf{T_{high\text{-}vs}}$), the error due to vertical sampling (denoted as $\mathbf{VSE^{L}}$, $\mathbf{VSE^{R}}$, and $\mathbf{VSE^{S}}$ respectively) can be quantified and the impact of vertical interpolation methods can be diagnosed.

This test results in 12 ensemble members for T and S respectively. Each ensemble member includes 24 fields from 1960 to 2017, which are used to quantify the time evolution of VSE. The spread across ensemble members provides an estimate for the uncertainty associated with the VSE.

2.2 Results

Here we provide some analysis of the VSE:

(1) Vertical structure of VSE

To test the impact of VSE on the vertical structure of the N^2 trend in Fig. 2, we calculate the linear trends of global averaged VSE from the surface to 2000m for the time period 1960 to 2017 in Extended Data Fig. 6. First, all vertical interpolation methods lead to negative error in the upper 30m, and a positive error for 30-100m. But below 100m, different interpolation methods lead to very different vertical structures, even different signs. Among the three methods, the RR method results in a weaker vertical fluctuation variation than two other methods, and is the most stable method. A spline results in the biggest vertical fluctuations, with a maximum error of ~7% near 450m. This is consistent with Cheng and Zhu [13] who used other gap-filling strategies. In this study, because the IAP data uses the RR method, we will focus on the results of RR (VSE^R).

For the RR method below 100m, the VSE^R is small and fluctuates around zero. The percentage of VSE^R is generally <3% from 20m to 500m, <1% within 500-1700 m, and <3% below 1700m (Extended Data Fig. 6b). This is much smaller than the N^2 percent changes exhibited in Fig. 2 (4~18% in the upper 150m, 2-6% within 220-500m, and 0-8% below 500m). This indicates that the N^2 structure presented in Fig. 2 is not biased by VSE^R and is reliable.

(2) Time evaluation of the VSE

To show the time evolution of the VSE and its impact on N^2 time variation (shown in Fig. 3 of the main manuscript), Extended Data Fig. 7 presents the time series of mean N^2 sampling error for 0-2000m.

There is a systematic bias in N^2 change due to vertical sampling, which is negative before 2005 and gets closer to zero after 2007 (Extended Data Fig. 7). This reveals the impact of time evolution of the ocean observation system. However, this bias is one order of magnitude smaller than the N^2 time series (Fig. 3). Quantitively, the spurious trends in VSE^R are less than <5% of the observed N^2 trend from 1960 to 2018 (the median bias is 1.9 [0.2, 4.3] %). Linear interpolation (VSE^L) is very similar to VSE^R, with a mean bias of 1.7 [0.1, 4.1] %. The spline is less biased than the other two methods and the trend bias is negative (-0.5 [-2.1, 0.9] %). Again, Spline is the least stable method, since its estimate is ill-posed by the vertical structure with the largest fluctuation, particularly for the positive errors within 400-500m.

In summary, we confirm with a “vertical subsample test” that VSE does not significantly bias the N^2 estimate in this study when using the IAP product (using Reiniger-Ross interpolation), but this error is non-negligible and should be taken into account in uncertainty estimates. Therefore, we have combined the results from vertical subsampling tests and the IAP mapping method to provide an estimate for the overall uncertainty of N^2 (see Methods section in the main manuscript and Supplementary Fig. 3 for an illustration).

The ensemble members of N^2 based on our ensemble approach are presented in Extended Data Fig. 10. Using the global metrics, it has a slightly positive bias (~0.1%) for the N^2 percent change of IAP estimate relative to the 1981-2010 average, within the 5-95% total uncertainty range of ~0.8%. Most of total uncertainty comes from the horizontal sampling and instrumental errors (~0.7%); the vertical sampling error (~0.2%) contributes to 1/4~1/3 to the total uncertainty.

Supplementary references:

1. Rhein, M. et al. Observations: Ocean. *In: Climate Change 2013: The Physical Science Basis. Contribution of Working Group I to the Fifth Assessment Report of the Intergovernmental Panel on Climate Change [Stocker, T.F., D. Qin, G.-K. Plattner, M. Tignor, S.K. Allen, J. Boschung, A. Nauels, Y. Xia, V. Bex and P.M. Midgley (eds.)].* Cambridge University Press, Cambridge, United Kingdom and New York, NY, USA (2013).
2. Ishii, M. & Kimoto, M. Reevaluation of historical ocean heat content variations with time-varying XBT and MBT depth bias corrections. *J. Oceanogr.* **65**, 287-299, doi:10.1007/s10872-009-0027-7 (2009).
3. Levitus, S. et al. World ocean heat content and thermosteric sea level change (0–2000 m), 1955–2010. *Geophys. Res. Lett.* **39**, doi:10.1029/2012GL051106 (2012).
4. Durack, P. J., Gleckler, P. J., Landerer, F. W. & Taylor, K. E. Quantifying underestimates of long-term upper-ocean warming. *Nat. Clim. Change* **4**, 999, doi:10.1038/nclimate2389 (2014).
5. Cheng, L. et al. Improved estimates of ocean heat content from 1960 to 2015. *Sci. Adv.* **3**, e1601545, doi:10.1126/sciadv.1601545 (2017).
6. Cheng, L., Abraham, J., Hausfather, Z. & Trenberth, K. E. How fast are the oceans warming? *Science* **363**, 128-129, doi:10.1126/science.aav7619 (2019).
7. Wang, G., Cheng, L., Abraham, J. & Li, C. Consensuses and discrepancies of basin-scale ocean heat content changes in different ocean analyses. *Clim. Dynam.* **50**, 2471-2487, doi:10.1007/s00382-017-3751-5 (2018).
8. Good, S. A., Martin, M. & Rayner, N. A. EN4: Quality controlled ocean temperature and salinity profiles and monthly objective analyses with uncertainty estimates. *J. Geophys. Res.* **118**, 6704-6716, doi:10.1002/2013JC009067 (2013).
9. Ishii, M. et al. Accuracy of global upper ocean heat content estimation expected from present observational data sets. *SOLA* **13**, 163-167, doi:10.2151/sola.2017-030 (2017)
10. Cheng, L., Wang, G., Abraham, J. & Huang, G. Decadal ocean heat redistribution since the late 1990s and its association with key climate modes. *Climate* **6**, 91, doi:10.3390/cli6040091 (2018).
11. Cheng, L. et al. Improved estimates of changes in upper ocean salinity and the hydrological cycle. *J. Clim.* submitted (2020).

12 Durack, P. J. Ocean salinity and the global water cycle. *Oceanography* **28**, 20-31, doi:10.5670/oceanog.2015.03 (2015).

13 Cheng, L. & Zhu, J. Uncertainties of the ocean heat content estimation induced by insufficient vertical resolution of historical ocean subsurface observations. *J. Atmos. Oceanic Technol.* **31**, 1383-1396, doi:10.1175/JTECH-D-13-00220.1 (2014).

14 Cheng, L. & Zhu, J. Benefits of CMIP5 multimodel ensemble in reconstructing historical ocean subsurface temperature variations. *J. Clim.* **29**, 5393-5416, doi:10.1175/JCLI-D-15-0730.1 (2016).

15 Allison, L. C. et al. Towards quantifying uncertainty in ocean heat content changes using synthetic profiles. *Environ. Res. Lett.* **14**, 084037, doi:10.1088/1748-9326/ab2b0b (2019).

16 Trenberth, K. E. et al. Observations: Surface and atmospheric climate change. Climate Change 2007: The Physical Science Basis, S. Solomon, et al., Eds., Cambridge University Press, 235–336 (2007).

17 Reiniger, R. F. & Ross, C. K. A method of interpolation with application to oceanographic data. *Deep Sea Res. pt.1* **15**, 185-193, doi: 10.1016/0011-7471(68)90040-5 (1968).

18 Lorenc, A. C., Bell, R. S. & Macpherson, B. The Meteorological Office analysis correction data assimilation scheme. *Quarterly Journal of the Royal Meteorological Society* **117**, 59-89, doi:10.1002/qj.49711749704 (1991).

19 Balmaseda, M. A., Mogensen, K. & Weaver, A. T. Evaluation of the ECMWF ocean reanalysis system ORAS4. *Q. J. Royal Meteorol. Soc.* **139**, 1132-1161, doi:10.1002/qj.2063 (2013).

Supplementary figures

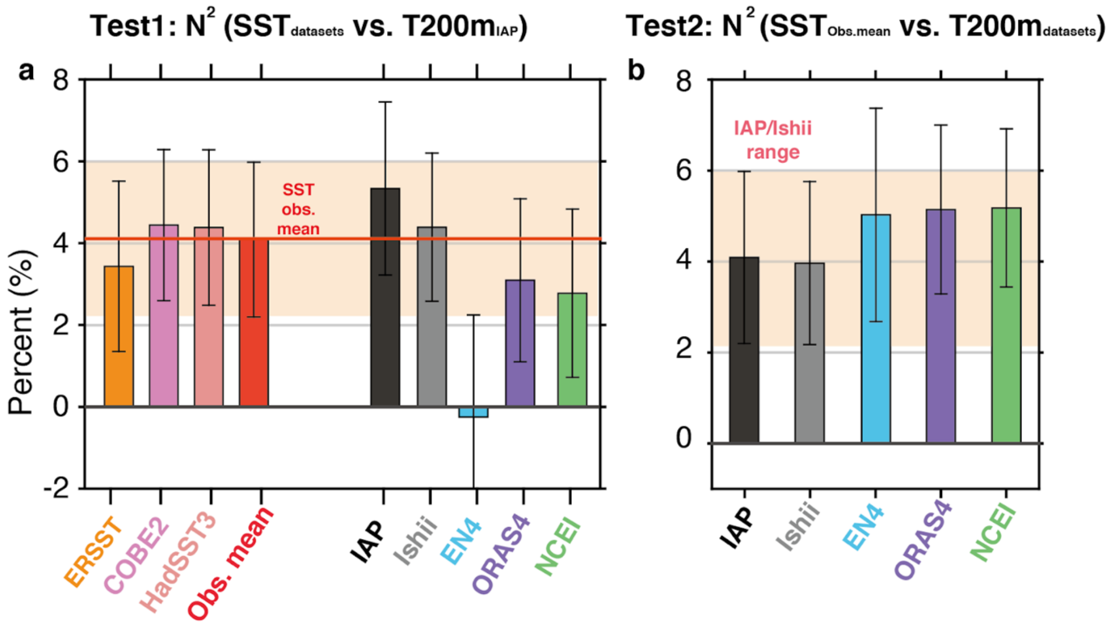

Supplementary Figure 1. Percent changes of N^2 within 1971-2010 period estimated by IPCC-AR5 method but using different data. In test-1 (**a**), Temperature at 200m (T200) is IAP data in all estimates with different SST data. In test-2 (**b**), SST data is observational mean (average over ERSST, COBE2, and HadSST3), but using different products for T200. The error bar denotes the 90% confidence interval (CI) of linear trend.

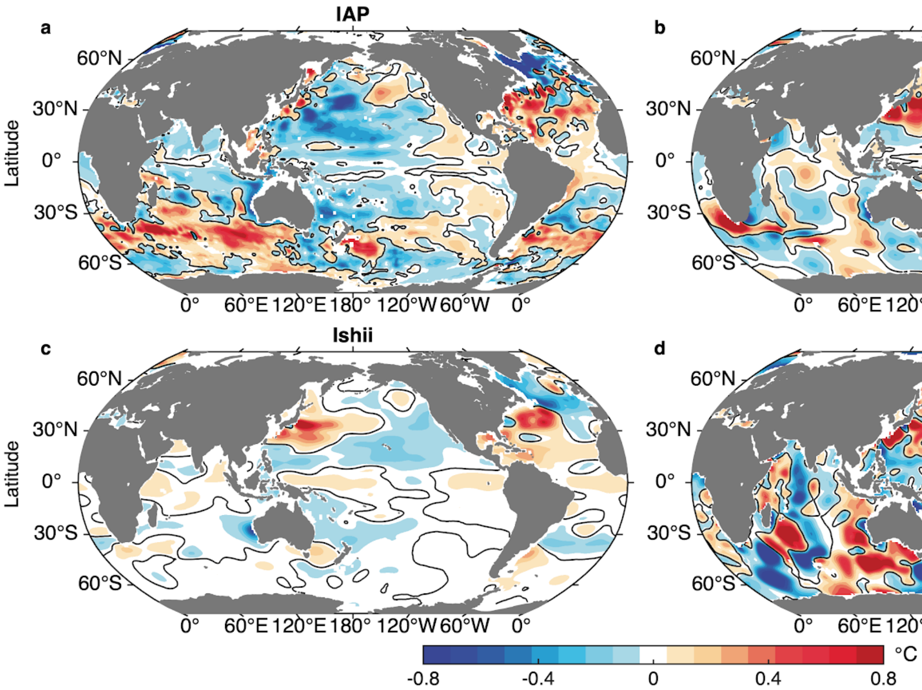

Supplementary Figure 2. An example showing the "conservative bias" in (b) EN4, (c) Ishii and (d) NCEI data diagnosed by calculating the annual temperature difference between 1990 and 1970 at 700m depth compared with the (a) IAP data. The contour shows zero anomaly.

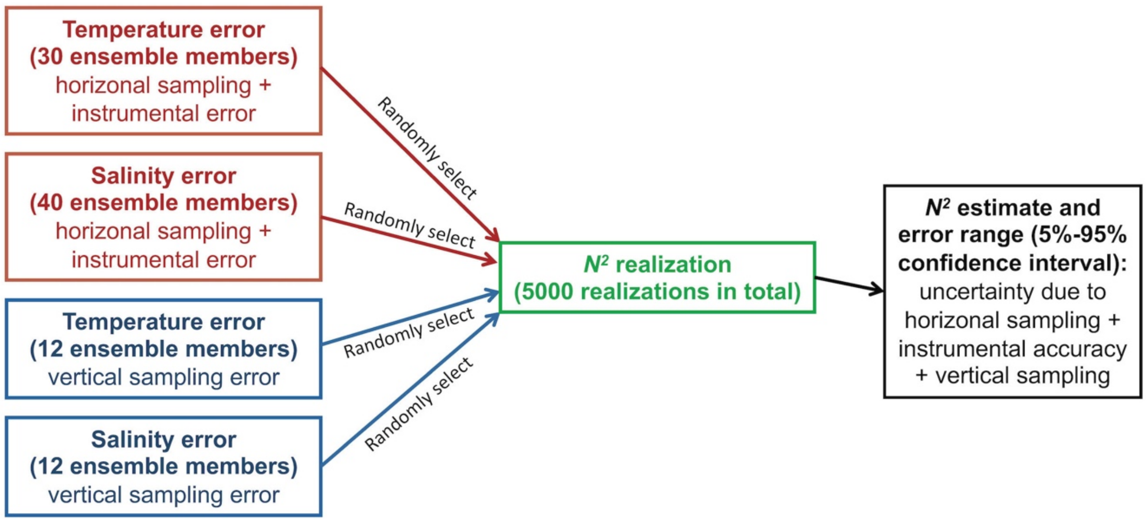

Supplementary Figure 3. A schematic showing the generation of total N^2 uncertainty by combining different error sources.

Supplementary Table 1. Climatological value (10^{-8} s^{-2}), linear trend (10^{-8} s^{-2} yr^{-1}) and the percent change (%) of N^2 for global and five major ocean basins during 1960-2018. Uncertainty range indicates 90% confidence interval (CI).

Basin		Global	Pacific	Atlantic	Indian	Southern	Arctic (65°-90°N)
Climatology		1687±39	2255±24	1659±49	2587±31	709±12	2352±200
IAP	**Trend**	1.5 [1.4~1.7]	2.1 [2.0~2.3]	1.2 [1.0~1.3]	1.6 [1.5~1.8]	1.0 [0.8~1.2]	2.1 [1.0~2.9]
	Percent	5.3 [5.0~5.8]	5.6 [5.2~5.9]	4.1 [3.5~4.6]	3.7 [3.4~4.2]	7.9 [6.8 ~9.6]	5.4 [2.6~7.4]
Ishii	**Trend**	1.6±0.4	2.0±0.6	1.6±0.4	2.3±0.4	0.7±0.1	2.0±0.4
	Percent	5.7±1.3	5.3±1.7	5.7±1.3	5.2±1.0	6.1±0.9	4.7±0.9
EN4	**Trend**	0.9±0.3	1.4±0.6	0.5±0.3	0.7±0.5	0.3±0.1	1.4±0.6
	Percent	3.0±1.0	3.5±1.5	1.8±0.9	1.7±1.1	2.9±1.1	3.5±1.5
ORAS4	**Trend**	1.1±0.3	1.6±0.7	0.7±0.4	2.5±0.7	0.2±0.2	-0.3±0.5
	Percent	3.7±1.2	4.2±1.7	2.4±1.6	5.8±1.6	1.9±1.2	-1.0±1.5
NCEI	**Trend**	1.3±0.3	1.8±0.7	0.9±0.5	1.7±0.7	0.6±0.2	3.9±3.6
	Percent	4.5±1.0	4.7±1.8	3.1±1.6	3.9±1.6	5.0±1.5	9.8±9.0

Supplementary Table 2. A summary of vertical levels and vertical interpolation methods used in different gridded products.

Datasets	Vertical levels	Vertical Interpolation method
IAP	41 (1-2000m)	Modified Reiniger and Ross (1968)[17]
NCEI	26 (0-2000m)	Modified Reiniger and Ross (1968)[17]
Ishii	28 (0-3000m)	Averaging data in grid-box regions (Ishii et al. 2017)[9]
EN4	31 (5-2134m)	The Analysis Correction (AC) scheme with nearest neighbor approach (Lorenc et al. 1991)[18]
ORAS4	31 (5-2134m)	3D-Var method based on the First-Guess at Appropriate Time (FGAT) approach (Balmaseda et al. 2013)[19]

Supplementary Table 3. Trends (10^{-8} s^{-2} yr^{-1}) and the percent changes (%) of N^2 during 1960-2018 for the total observed change, and temperature and salinity contributions. Uncertainty range is 90% CI.

Basin		Global	Pacific	Atlantic	Indian	Southern	Arctic (65°-90°N)
All	Trend	1.5 [1.4~1.7]	2.1 [2.0~2.3]	1.2 [1.0~1.3]	1.6 [1.5~1.8]	1.0 [0.8~1.2]	2.1 [1.0~2.9]
	Percent	5.3 [5.0~5.8]	5.6 [5.2~5.9]	4.1 [3.5~4.6]	3.7 [3.4~4.2]	7.9 [6.8~9.6]	5.4 [2.6~7.4]
T-only	Trend	1.5 [1.4~1.6]	1.8 [1.7~1.8]	1.9 [1.8~2.0]	1.8 [1.7~1.8]	1.1 [1.0~1.2]	0.4 [0.3~0.4]
	Percent	5.2 [5.0~5.4]	4.6 [4.5~4.8]	6.7 [6.5~7.0]	4.0 [3.8~4.2]	8.0 [7.2~8.6]	1.0 [0.7~1.1]
S-only	Trend	0.0 [-0.0~0.2]	0.4 [0.2~0.5]	-0.8 [-0.9~-0.6]	-0.1 [-0.3~0.1]	-0.0 [-0.1~0.3]	1.7 [0.7~2.5]
	Percent	0.1 [-0.1~0.5]	0.9 [0.6~1.2]	-2.7 [-3.3~-2.2]	-0.2 [-0.6~0.2]	-0.1 [-0.7~2.0]	4.5 [1.7~6.5]

Supplementary Table 4. Trends (10^{-8} s^{-2} yr^{-1}) and the percent changes (%) of N^2 at upper 2000m during 1960-2018 by using different climatology fields based on IAP analysis. The uncertainty range is 90% CI.

Basin		Global	Pacific	Atlantic	Indian	Southern	Arctic (65°-90°N)
1981-2010	**Trend**	1.5 [1.4~1.7]	2.1 [2.0~2.3]	1.2 [1.0~1.3]	1.6 [1.5~1.8]	1.0 [0.8~1.2]	2.1 [1.0~2.9]
	Percent	5.3 [5.0~5.8]	5.6 [5.2~5.9]	4.1 [3.5~4.6]	3.7 [3.4~4.2]	7.9 [6.8~9.6]	5.4 [2.6~7.4]
1961-1990	**Trend**	1.5 [1.4~1.7]	2.1 [2.0~2.3]	1.1 [1.0~1.3]	1.6 [1.5~1.8]	1.1 [0.9~1.3]	2.1 [1.0~2.9]
	Percent	5.4 [5.1~5.9]	5.7 [5.3~6.0]	4.1 [3.5~4.7]	3.8 [3.4~4.3]	8.1 [7.0~9.6]	5.6 [2.7~7.6]
1971-2000	**Trend**	1.5 [1.4~1.7]	2.1 [2.0~2.3]	1.1 [1.0~1.3]	1.6 [1.5~1.8]	1.1 [0.9~1.3]	2.1 [1.0~2.9]
	Percent	5.6 [5.0~5.8]	5.8 [5.3~6.0]	4.3 [3.5~4.7]	4.0 [3.4~4.2]	8.2 [6.9~9.5]	5.5 [2.7~7.5]
1991-2018	**Trend**	1.5 [1.4~1.7]	2.1 [2.0~2.3]	1.1 [1.0~1.3]	1.6 [1.5~1.8]	1.0 [0.8~1.2]	2.1 [1.0~2.9]
	Percent	5.3 [4.9~5.7]	5.5 [5.2~5.8]	4.0 [3.4~4.6]	3.7 [3.3~4.2]	7.9 [6.7~9.5]	5.4 [2.6~7.4]